AIMS Geosciences, 5 (1): 41–65.
DOI: 10.3934/geosci.2019.1.41
Received: 10 November 2018
Accepted: 07 March 2019
Published: 27 March 2019

http://www.aimspress.com/journal/geosciences

Research article

Stable isotope ratios and speleothem chronology from a high-elevation alpine cave, southern San Juan Mountains, Colorado (USA): Evidence for substantial deglaciation as early as 13.5 ka

Ray Kenny*

Research Geologist, Durango, CO-81301, USA

*** Correspondence:** Email: kennyphdpg@gmail.com; Tel: 9702599509.

Abstract: Deglaciation ages for valley glaciers from the last glacial maximum are difficult to obtain with precision. The unequal or non-uniform loss of glacial ice cover (spatial heterogeneity) during glacial retreat results in exposure of considerable land surface area prior to complete deglaciation. New U-series dates from an 11cm long stalagmite in a shallow, high elevation (3242 m) cave in the southern San Juan Mountains of southwestern Colorado (USA), indicate that substantial, high-elevation glacial ice ablation occurred prior to 13.5 ka. The stalagmite dates compare well with other deglaciation studies in central and southern Colorado that show deglaciation occurred between ca. 13 ka to 15 ka. Low $\delta^{13}C$ values from 13.5 ka speleothem growth bands, relative to the $\delta^{13}C$ value of the host carbonate, suggest that alpine plant and soil cover was established at this location, aspect, and elevation prior to 13.5 ka. Calcite luminescence in the 13.5 ka growth bands indicates the presence of humic and fulvic acids released by the roots of living plants and decomposition of vegetative matter. The carbon isotope ratios, calcite luminescence, and U-series dates suggest that the southern San Juan Mountains, at this high elevation site and southern aspect were substantially ice-free prior to 13.5 ka.

Keywords: San Juan Mountains; U-series; speleothem; deglaciation timing; Last Glacial Maximum; Colorado

Abbreviations: SSJM: Southern San Juan Mountains; CN: Cosmogenic Nuclides; amsl: above mean sea level; m: meters; mm: millimeters; ft: feet; in: inches; yr: year; ka: kilo annum; NOAA: National Oceanic and Atmospheric Administration; USDA-NCS-SNOTEL: US Department of Agriculture-Natural Resources Conservation Service-Snow Telemetry; TIMS: thermalionization mass spectrometry; LGM: Last Glacial Maximum; MIS: Marine Isotope Stage; UV: Ultra-violet; SWUV: Short-wave Ultra-violet; HA: Humic acids; FA: Fulvic acids; YD: Younger Dryas; ITCZ: Intertropical Convergence Zone; MAAT: mean annual air temperature; GRIP: Greenland Ice Core Project; D-fabric: Dendritic fabric; C-fabric: Compact columnar fabric

1. Introduction

Only a few methods are presently available for obtaining quantitative data on the timing, location and evolution of glacial ice cover throughout the deglaciation process in high-relief terrain. Previous quantitative Quaternary climate studies in the southwestern and central mountains of Colorado (USA) have predominantly focused on radiocarbon ages, palynology and cosmogenic nuclides (CN) [1–12]. Quantitative terrestrial climate records for the southern San Juan Mountains (SSJM) of Colorado are sparse and no previous U-series dates on speleothems from high-elevation caves have been reported for this area.

Numerous studies have established that U-series dates from speleothems provide precise, high-resolution data yielding uncertainties of less than 0.5% [13,14]. A thorough and detailed review of U-series speleothem dating is provided by Richards and Dorale [15] and Asmerom [16]. U-series dating of stalagmites from alpine caves are scarce but have provided insight into high-elevation climate change, glacier evolution and palaeotemperature fluctuations [17].

Hendy [18] established the methodology for analyzing stable isotope ratios of speleothems and their applicability for use as palaeoclimate indicators. Oxygen isotope ratios of stalagmites from high alpine caves have been correlated to unstable climate conditions recorded in ice cores [17,19,20] and have been used to detail the timing of monsoon strengthening in Asia with increasing temperatures in Greenland at the start of the Holocene [21]. Carbon isotope ratios of speleothems are sensitive to plant cover variations and have been used to track changes in C_3 and C_4 plant pathways through time [13]. Carbon and oxygen isotope ratios of stalagmites have been shown to accurately document both long- and short-term climate variability [13,17,22–26] and have been successfully used to recognize changes in, and the presence of, surface plant cover [13,27,28].

2. Study site

The SSJM cave is located approximately 55 (linear) kilometers north of Durango, Colorado (USA) in the upper Animas River drainage of southwestern Colorado (Figure 1) near a broad glacial divide (Molas Pass, elevation 3233 m). The shallow, joint-controlled, speleothem-poor cave is developed in limestone strata of the Pennsylvanian Hermosa Group and terminates in a siliciclastic-rich, bedding-plane breakdown room. The calcite stalagmite was located approximately 300 m from a narrow joint-controlled cave entrance. The cave entrance is at an elevation of approximately 3242 m (amsl). The sedimentary rock layers of the Hermosa Group at the study site

dip ~10–12º to the south-southwest and the land surface is dissected by headwater tributaries that drain down dip. Swales, shallow depressions and natural ponds define the surface topography above the cave passageways.

Glacial ice thickness for this elevation, location, and aspect during the Last Glacial Maximum (LGM) is not precisely known. Nearby glacial striations and grooves are a testament to the presence of glacial ice from the LGM. During the LGM the SSJM were covered by a 5000 km^2 regional ice cap (Figure 2) [29–31]. Numerous (non-glaciated) mountain peaks in the SSJM exceed 4200 m. The majority of north-facing cirque floors occur at an elevation of around 3700 m [1]. The average elevation of north-facing cirque floors is ~450 m higher than the land surface directly above the cave entrance. From these data, and early map work done by Atwood and Mather [29], it is inferred that the study area would have been ice covered during the LGM (Figure 2). Valley glaciers during the LGM extended down to an elevation of ~1995 m (amsl), ~55 (linear) kilometers south of the study site.

The SSJM of southwestern Colorado have very few alpine caves and most are small in size [32]; even fewer contain speleothems. Finding stalagmites suitable for palaeoenvironmental or palaeoclimate research in high-elevation alpine caves is uncommon. When high-elevation stalagmites are present, they are typically smaller in size relative to low-elevation, warm climate caves [17,33]. The author and other cavers have surveyed countless small caves in the SSJM for well over a decade. To date, only one cave passage in the SSJM contained a stalagmite suitable for U-series dating. As such, no other stalagmites have been located to corroborate the Th/U dates presented herein. Active precipitation of carbonate in the study cave is mostly limited to a few stalactites, minimal flowstone, and a few soda straws in the bedding-plane, break-down room. Modern surface vegetation above the cave system consists of open subalpine vegetation (*Artemisia spp*. and *Poaceae spp*.) and patches of Dwarf Willow (*Salix spp*) and *Carex* (*spp*) bordering minor and sporadic wetlands and lakes. Scattered stands of Engelmann Spruce (*Picea engelmannii)* and subalpine Fir (*Abies lasiocarpa*) dominate the subalpine forest zone. At an elevation of 3242 m (~10,637 ft) modern soil temperature regimes are predominantly cryic. Soil orders vary from inceptisols (on steep slopes), to spodosols (associated with acidic forest cover), to locally intermittent mollisols, and histosols associated with low-lying bogs and fens; effective rooting depths on the limestone bedrock vary between 175–500 mm (~7–20 in).

Current climate conditions in the low latitude SSJM are changing rapidly. The SSJM of Colorado warmed ~1.1 ºC (~2 °F) between 1977 and 2007 [34,35]. From 1978–2004 snowmelt in the SSJM has already shifted ~2 weeks earlier [36,37]. Longer term records from NOAA cooperative stations and USDA-NRCS-SNOTEL stations (from 1961–1990) indicate that the annual average precipitation near the study site likely ranges between 109 to 120 cm/yr. Approximate January temperatures (Molas Pass SNOTEL records from 1988–2018) range between −8.6 to −9.6 ºC (~16.5–14.7 °F); July temperatures range between 9.3–10.8 ºC (~48–51 °F).

3. Research hypothesis

In stalagmites, calcite U-series ages coupled with analyses of calcite oxygen and carbon isotope ratios have been universally and successfully used to: (1) determine the onset of stalagmite growth

and carbonate growth intervals; and, (2) better understand climate and environmental variability during the stalagmite growth intervals. This research was initially undertaken to: (1) determine the onset of stalagmite growth; and, (2) use oxygen and carbon isotope ratios along carbonate growth intervals as proxies for insight into palaeoclimate and palaeoenvironmental conditions.

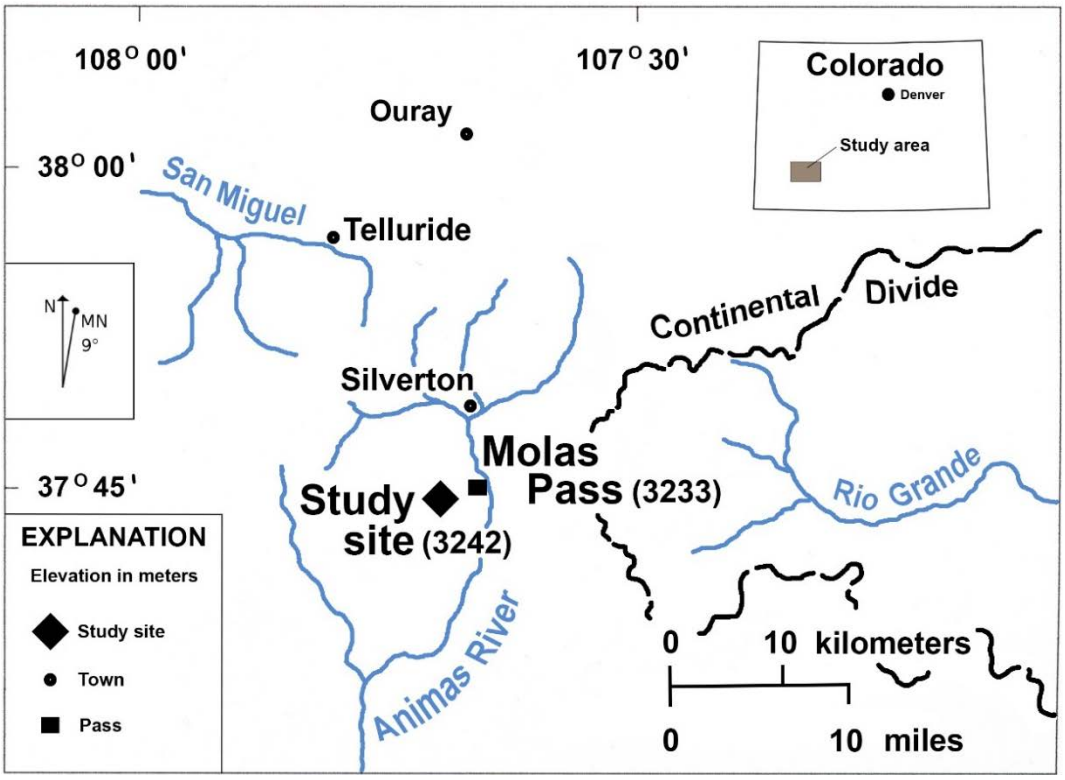

Figure 1. San Juan Mountains Colorado (USA) and selected towns (circles) and passes (squares) discussed in this study. The approximate location of the Continental Divide is shown by the dashed lines. Approximate location of the SSJM cave entrance (diamond) is ~55 linear kilometers north of Durango, Colorado (USA), and ~2.3 km west of Molas Pass. Exact coordinates for the cave entrances have not been provided as per a request from the USDA Forest Service.

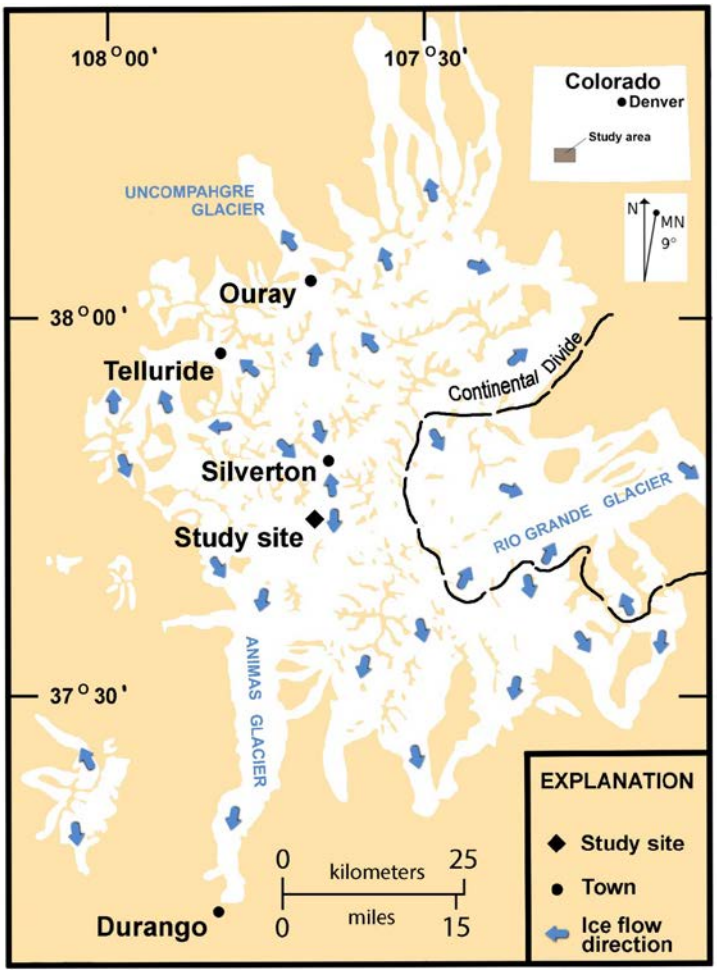

Figure 2. The SSJM were extensively glaciated and covered by a 5000 km^2 ice cap during the LGM [31]. The approximate location of the Continental Divide is shown by the dashed lines. The ice fields, valley glaciers and numerous cirques (white) cover a linear distance of ~120 km from the northernmost terminal moraine to the southernmost terminal moraine of the Animas Glacier (Durango, Colorado). Arrows (blue) indicate the direction of glacier ice flow determined from glacial striations, alpine cirque aspects, boulder deposits, regional mountain divides, the continental divide, maturely dissected U-shaped valleys notably sculpted by ice action, terminal and recessional moraines, and general elevation changes. Figure modified from [29,38].

4. Methods

Only one stalagmite from this unique, high-elevation cave was sampled for geochemical analyses due to the paucity of speleothems in the cave; no other caves in the SSJM have yielded suitable stalagmites. The stalagmite was located in a horizontal cave passage approximately 300 m from the cave entrance at an active drip-water site. The cave entrance is ~4.0–4.5 m below the land surface; we assumed a similar depth at the speleothem sample site inside the cave. The intact stalagmite formed in-place, directly on bedrock carbonate of the Pennsylvanian Hermosa Group and

a portion of the bedrock base was collected with the sample to ensure that a representative basal age was obtained.

In the laboratory, the 11cm long stalagmite was cut parallel to the growth axis with a diamond saw. Half of the sectioned stalagmite (Figure 3) was sent to the University of Texas at Austin where age determinations were conducted using U-series isotope measurements. Long transects along continuous growth bands were sampled to ensure accuracy followed by chemical separation of U, Th, and Pa; measurements of U-series isotopes by thermal ionization mass spectrometry (TIMS) were used to establish stalagmite ages. Samples for U-series measurements were obtained along continuous growth bands to avoid areas where possible calcite recrystallization may have occurred which could have resulted in possible U loss. The extraction and analysis procedure is described in detail by Musgrove et al [39]. Samples for carbon and oxygen isotope ratios were drilled along the central axis of the stalagmite (Figure 3) and along the oldest growth layer using a diamond drill bit. To test for oxygen isotope equilibrium conditions (Hendy Test), samples were obtained along a single growth layer [18]. Isotopic disequilibrium can result from kinetic fractionation during rapid escape of CO_2 or evaporation [40]. If ^{18}O values along a single growth layer are consistent (i.e., <0.8‰ change) the carbonate is generally considered to be in isotopic equilibrium [18,41]. Half of the sectioned stalagmite was stimulated with UV light in a controlled environment (UV light-box) to test for calcite luminescence. Carbon and oxygen isotope ratios were obtained from the Colorado Plateau Stable Isotope Lab at Northern Arizona University (Flagstaff, AZ) and at the Center for Stable Isotope Mass Spectrometry at the University of Texas at Austin (TX). UV light stimulation, XRD analyses and thin section preparation and analyses were completed at Fort Lewis College (Durango, CO).

5. Results

Three U-series dates (Table 1) were obtained on the 11cm long stalagmite from the SSJM cave (Figure 3). The U-series dates indicate a complex, episodic growth history for the SSJM stalagmite wherein periods of rapid calcite precipitation were separated by a period of interrupted growth. Approximately 86% of stalagmite growth occurred within a timespan of only a few hundred years, between 13.446 ± 0.170 to 13.284 ± 0.180 Th/U ka. This was followed by a significant hiatus of ~10,000 years; speleothem precipitation resumed around 2.666 ± 0.503 ka. The cause of the significant hiatus could not be fully determined by this study. Renewed stalagmite growth at ~2.666 ± 0.503 Th/U ka coincides with an episode of increased effective moisture in the southwestern USA which occurred ~3 ka to 8×10^{-1} ka [42]. The older stalagmite dates compare well with other deglaciation studies in central and southern Colorado that suggest all western USA mountains were glacier-free by ca. 13 ka to 15 ka [12].

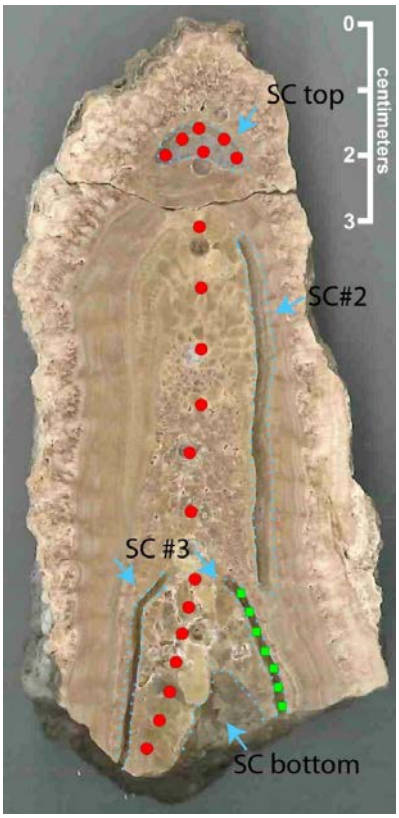

Figure 3. Sectioned stalagmite is 11cm long. Long transects (small blue dots) along continuous growth bands were used to obtain the most accurate U-series ages. The location of the SC#2 continuous growth band sample (not along the outermost bounding layer) was selected to avoid contact with apparent calcite layer irregularities close to the edge of the bounding layer. U-series dates: SC top = 2.666 ± 0.503 ka growth band; SC#2 = 13.284 ± 0.180 ka growth bands; SC#3 = 13.446 ± 0.170 growth band. Samples for carbon and oxygen isotope ratios were drilled along the central axis (red circles) and along a continuous growth layer (green squares, SC#3) to test for oxygen isotope equilibrium conditions (Hendy Test).

Table 1. Measured U-series data for the SSJM cave stalagmite.

U-series data	SC top (2.666 ± 0.503 ka)	SC#2 (13.284 ± 0.180 ka)	SC#3 (13.446 ± 0.170 ka)
Depth (mm)	17.5 ± 2.5	27 ± 1	100 ± 5
^{238}U (ppb)	1029 ± 70	2073 ± 11	2322 ± 7
^{232}Th (ppt)	70648 ± 335	23743 ± 67	11051 ± 39
^{230Th232}Th (atomic $\times 10^{-6}$)	49 ± 1	215 ± 1	544 ± 5
d^{234}U (measured)	6694 ± 968	273 ± 4	338 ± 4
$^{230Th}/^{238}$U (activity)	0.2040 ± 0.0143	0.1491 ± 0.0012	0.1569 ± 0.0014
d$^{234}U_{initial}$ (corrected)	6745 ± 975	283 ± 5	351 ± 4
Th/U age (ka)	2666 ± 503	13284 ± 180	13446 ± 170

Hendy test results (oxygen isotope equilibrium conditions) on the 13.446 ± 0.170 ka growth lines (Figure 3) indicate that calcite precipitation likely occurred under isotopic equilibrium conditions; $\delta^{18}O$ values along the single growth layer varied by only 0.35‰ (Figure 4), which is less than the variance of <0.8‰ established by Hendy [18]. No significant variation in ^{18}O composition was observed on a plot of oxygen isotope ratios versus stalagmite age (Figure 5). Average oxygen isotope values for the younger 2.666 ± 0.180 ka growth bands were −10.0 ± 0.1‰$_{VPDB}$ (n = 6); average oxygen isotope values for the older 13.446 ± 0.170 and 13.284 ± 0.180 ka growth bands were −10.3 ± 0.1‰$_{VPDB}$ (n = 13; Table 2).

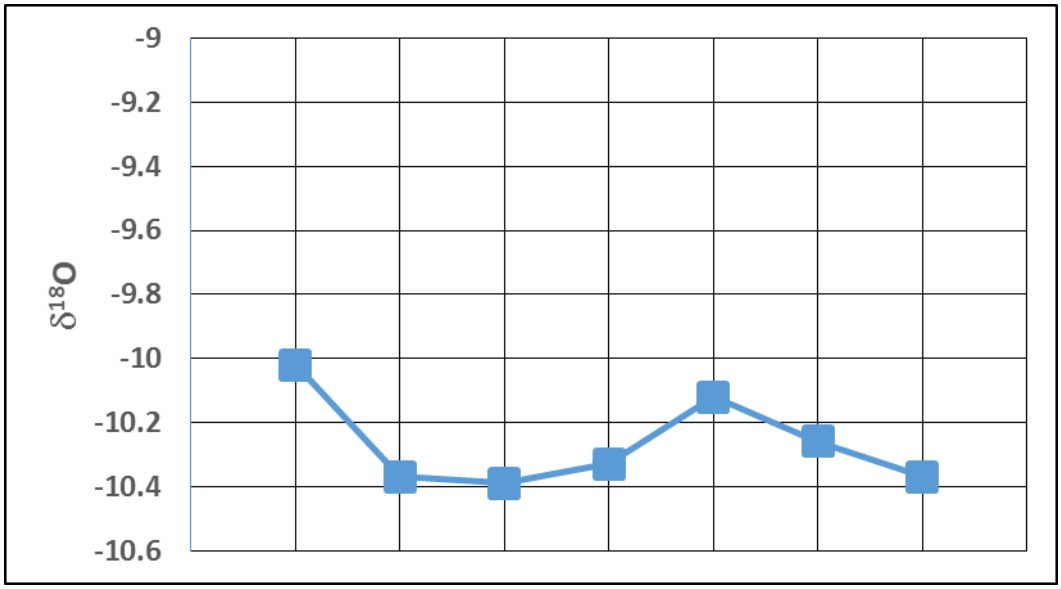

Figure 4. Hendy test results indicates that calcite precipitation occurred under isotopic equilibrium conditions; $\delta^{18}O$ values along a single growth layer (13.446 ± 0.170 ka) varied by 0.35‰, which is less than the established variance of <0.8‰.

Carbon isotope values in the stalagmite carbonate were plotted relative to carbon isotope values of the host carbonate (Table 2; Figure 6). Low $\delta^{13}C$ values in the speleothem precipitate, relative to the Pennsylvanian Hermosa Group host carbonate, likely reflect the oxidation of local organic matter and suggest that some soil layer and alpine plant cover was present at the surface, at this elevation (~3242 m) and southern aspect, by 13.5 ka.

The sectioned stalagmite was stimulated by short-wave ultra-violet (SWUV) light. The stalagmite photoluminesced light green (Figure 7) and the oldest growth bands (13.5 ka) strongly luminesced; some layers had reduced luminescent brilliance due to clay and other colored inclusions. Researchers have shown that the strongest sources of luminescence in most conventional vadose stalagmites is produced by organic impurities, specifically calcium salts of humic acids (HA) and fulvic acids (FA) derived from soils above the cave [43–46]. These acids are released by the roots of living plants and by the decomposition of dead/decaying vegetative matter [45–49]. Strong luminescence in the oldest growth bands, likely caused by HA and FA, similarly suggests that some soil layer and alpine plant cover was already present at the surface by 13.5 ka.

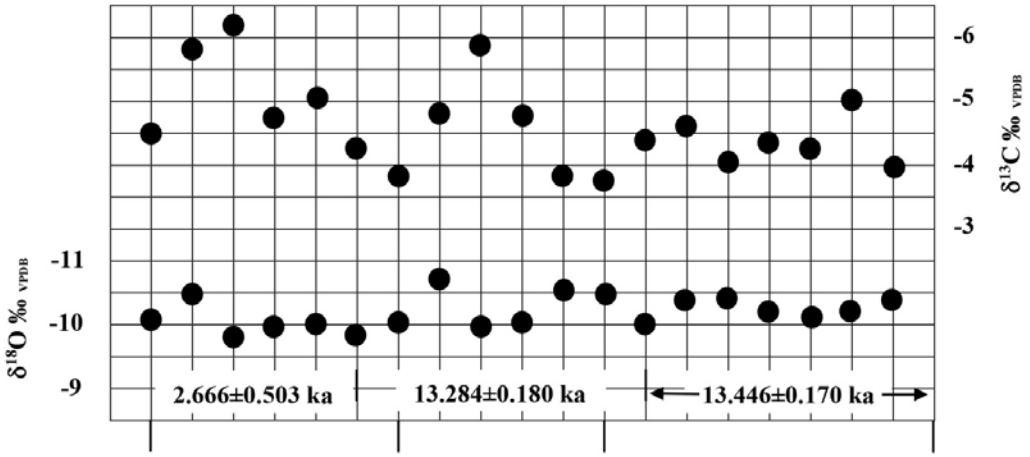

Figure 5. Stable isotope data versus stalagmite age. Oxygen and carbon isotope values are shown with circles. No significant variation in average $\delta^{18}O$ values was observed between the 2.666 ± 0.503 ka stalagmite segment (av = −10.0 ± 0.1‰; n = 6), and the 13.446 ± 0.170 and 13.284 ± 0.180 ka stalagmite segments (av = −10.3 ± 0.1‰; n = 13). $\Delta^{13}C$ values trend toward slightly lower ^{13}C values in the 2.666 ± 0.503 ka stalagmite segment (av = −5.1 ± 0.1‰), but vary by less than 1‰ relative to the 13.446 ± 0.170 ka and 13.284 ± 0.180 ka growth bands (av = −4.4 ± 0.1‰).

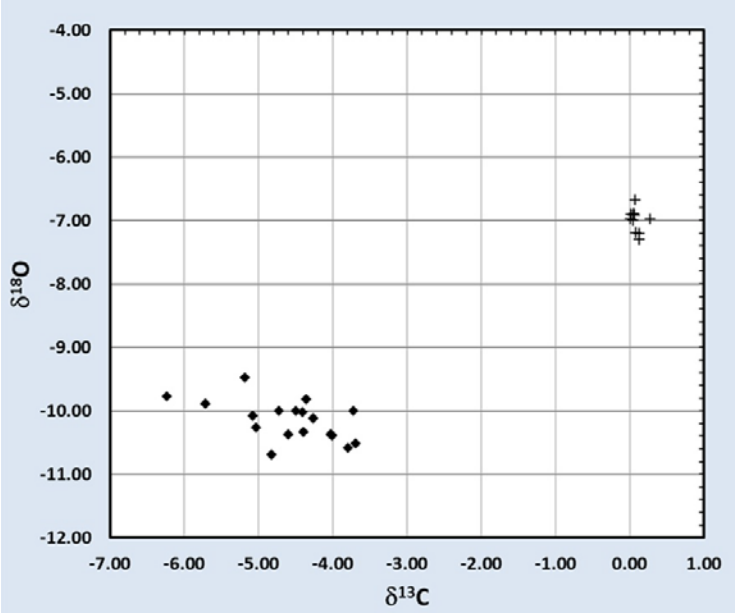

Figure 6. Stable isotope values for the host carbonate (Hermosa Group; n = 11; crosses) versus stalagmite isotope values (n = 19; diamonds). $\delta^{13}C$ values in the stalagmite are notably lower relative to $\delta^{13}C$ values of the host carbonate. Soil-derived CO_2 is the only likely source of low ^{13}C and the $^{13}C/^{12}C$ ratios indicate the presence of some soil-CO_2/vegetative cover by 13.446 ± 0.170 ka.

Table 2. SSJM cave stalagmite calcite and Hermosa Group carbonate carbon (±0.1‰$_{VPDB}$) and oxygen (±0.1‰$_{VPDB}$) isotope data.

$\delta^{13}C_{VPDB}$ (‰)	Average $\delta^{13}C_{VPDB}$ (‰)	$\delta^{18}O_{VPDB}$ (‰)	Average $\delta^{18}O_{VPDB}$ (‰)	SSJM cave stalagmite segments and Hermosa Carbonate descriptions
−4.03		−10.37		13.446 ± 0.170 ka segment
−5.04		−10.26		13.446 ± 0.170 ka segment
−4.27		−10.12		13.446 ± 0.170 ka segment
−4.40		−10.33		13.446 ± 0.170 ka segment
−4.01		−10.39		13.446 ± 0.170 ka segment
−4.60		−10.37		13.446 ± 0.170 ka segment
−4.41	−4.4	−10.02	−10.3	13.446 ± 0.170 ka segment
−3.70		−10.51		13.284 ± 0.180 ka segment
−3.80		−10.58		13.284 ± 0.180 ka segment
−4.77		−10.03		13.284 ± 0.180 ka segment
−5.72		−9.9		13.284 ± 0.180 ka segment
−4.83		−10.69		13.284 ± 0.180 ka segment
−3.73	−4.43	−10.01	−10.3	13.284 ± 0.180 ka segment
−4.36		−9.82		2.666 ± 0.503 ka segment
−5.08		−10.08		2.666 ± 0.503 ka segment
−4.73		−10.00		2.666 ± 0.503 ka segment
−6.24		−9.77		2.666 ± 0.503 ka segment
−5.87		−10.54		2.666 ± 0.503 ka segment
−4.53	−5.1	−10.07	−10.0	2.666 ± 0.503 ka segment
0.13		−7.31		Hermosa Group*
−0.07		−6.91		Hermosa Group
0.06		−6.90		Hermosa Group
0.08		−7.20		Hermosa Group
−0.28		−6.98		Hermosa Group
0.7		−7.10		Hermosa Group
0.2		−7.31		Hermosa Group
−0.1		−7.11		Hermosa Group
0.25		−7.25		Hermosa Group
−0.07		−6.22		Hermosa Group
0.07	0.1	−6.69	−7.0	Hermosa Group
				*All Hermosa Group outcrop samples collected ~200–400 m from the cave entrance

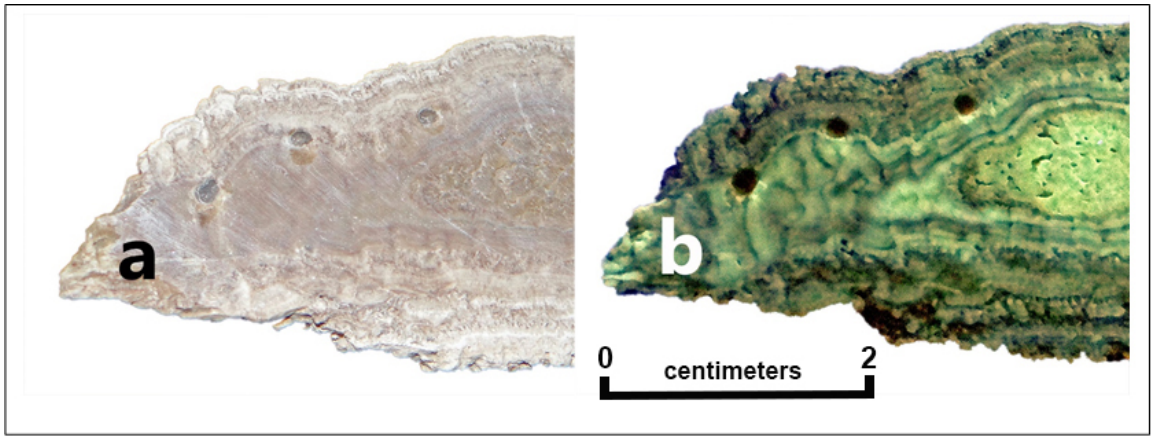

Figure 7. (a) Sectioned stalagmite under plane light; (b) same stalagmite exposed to UV light. Stalagmite luminesces a pale green (prominent luminescence in central part of stalagmite is within the ~13.5 ka stalagmite segment); darker areas may be clay-rich [45,47].

6. Discussion

6.1. Stalagmite growth layers and palaeoclimate

U-series dates on the SSJM cave stalagmite accurately record the onset of calcite precipitation at ~13.5 ka. Stalagmite growth was initiated during the warm and moist Bølling/Allerød interstadial (~14.7 ka–12.9 ka; [50]). The majority of stalagmite growth precipitated during the third quarter of this climatic optimum followed by a significant growth hiatus after ~13.3 ka. Effective (atmospheric) moisture increased from the Gulf of Mexico into southwestern USA during the Bølling/Allerød interstadial [51]. This influx of effective moisture and warm temperatures: (1) likely helped accelerate the rate of deglaciation; and/or, (2) provided the moisture needed to maintain the constant seepage rate needed for speleothem growth. Rapidly rising northern hemisphere summer insolation [52], higher atmospheric levels of CO_2, and an increase in rainfall appear to have accompanied deglaciation and rapid retreat of mountain glaciers in many areas of the world [53–55]. How these climate dynamics may have impacted the mid latitude continental regions is only now becoming better understood [56,57], and it appears likely that an increase in convective rainfall may also have accompanied or accelerated the retreat of mid latitude mountain glaciers. Given that the SSJM region was impacted by a significant increase in effective moisture after the LGM termination, then an increase in the volume of drip water could have contributed to a constant flow of drip water to the stalagmite. A constant seepage rate could have been maintained from either: (a) a direct increase in effective moisture during the Bølling/Allerød interstadial; and/or, (b) remnant glacial meltwater filtering down from the higher peaks adjacent to the study site via seepage into the numerous fractures, faults, and bedding plane horizons that crisscross this mountainous terrain.

Cessation of stalagmite growth occurred just prior to the onset of the Younger Dryas (YD) cooling episode (~12.9–11.5 ka; [58]). Rapid onset of the YD cooling episode likely affected the high-elevation climate zones of the SSJM earlier than lower elevation environments. If this

supposition is correct, cessation of stalagmite growth at ~13.284 ± 0.180 ka may represent the beginning of the YD cooling episode (~12.9 ka) in the higher elevations of the SSJM. It is also possible that the significant growth hiatus observed in the stalagmite was triggered by other causes. (1) A change in the local percolation pathways due to faulting and seismic activity [59,60]. Growth perturbations in stalagmites due to large-scale earthquakes have been recorded in areas known for prolonged seismic activity [60]. Notable stalagmite anomalies due to seismic activity include abrupt and conspicuous tilting, breakage, or rotation of growth axes followed by regrowth if the percolation pathway has not shifted or become blocked. These distinctive seismically-induced features, were not observed in the SSJM stalagmite. (2) Drip water became under-saturated (with respect to the stalagmite's calcite or aragonite) which halted calcite precipitation and may also have dissolved pre-existing stalagmite growth layers [61]. Hiatuses due to chemical erosion from under-saturated drip waters often result from a significant *increase* in the volume or flux of drip water which occurs during times of greater than normal precipitation [61]. Evidence supporting surging cave or gushing drip waters capable of calcite corrosion may include: (a) larger detrital material entrapped along bounding calcite layers; and/or, (b) stair-step-like surfaces (micro-pits, micro-caves and micro-mesas) along calcite truncation surfaces referred to as "E" (erosion) layers observed under higher resolution [61]. No definitive E layer features were identified in ~13.284 ± 0.180 ka bounding layer. (3) It is also well-established that "drip-type" speleothem growth is often episodic [62]. Hence, calcite blockage or a change in the ceiling drip location could result in cessation of speleothem growth. Neither a change in the cave drip location nor a change in the location of surface water channels above the cave drip site can be ascertained with any certainty. Numerous other atmospheric, climate, physicochemical, and erosional possibilities could have contributed to growth cessation. Ultimately the causal mechanism leading to cessation of stalagmite growth is unknown and is beyond the scope of this study.

Renewed stalagmite growth at ~2.7 ka likely records a prominent event that remarkably coincides with the onset of an episode of increased effective moisture in the SSJM. Studies on cave deposits in the Guadalupe Mountains (New Mexico, USA; ~700 km east-southeast of this site) have shown that a "present day-like" climate existed in the southwestern USA between 4 ka and 3 ka [30,31,56,57,63,64], and that a "distinctly" wetter and cooler climate existed in the southwestern USA from 3 ka to 8×10^{-1} ka [63]. The onset of a wetter climate in the southwestern and western USA was likely due to the northward migration of the Intertropical Convergence Zone (ITCZ) which brought increasing rainfall to the lower latitude areas of the Northern Hemisphere [64]. A wetter, cooler climate commencing ~3 ka, correlates reasonably well with the onset of renewed stalagmite growth in the SSJM cave (at ~2.7 ka). Polyak and Asmerom [63] further showed that the middle Holocene climate in the southwestern USA *prior* to the climatic optimum (between 4ka and 3ka), was considerably drier. Palaeoecological changes in the SSJM have been predominantly influenced by large-scale climate trends. Pollen records preserved in a nearby lake (~1.5 km northeast of the cave at an elevation of 3325 m) showed an increase in effective moisture commencing ~2.6 ka [8]. Owing to the remarkable temporal correlation between speleothem growth and the well-documented climate shifts in the southwestern USA and the SSJM (~2.6 ka), it is plausible to suggest that reactivation of speleothem growth (at ~2.7 ka, at the same ceiling drip location) predominantly occurred due to the increase in effective moisture in the southwestern USA and in the high-alpine

environment of the SSJM. Nevertheless, the possibility exists that the ceiling drip was reactivated, at the same location, by other processes such as a change in the surface water hydrology. Multiple speleothem analyses would be needed to confirm that an increase in effective moisture triggered reactivation of speleothem growth at ~2.7 ka. At the time of this writing, no other caves with stalagmites have been located in the SSJM and no such corroborating spelean data is available.

6.2. U-series dates and stable isotopes

The growth of stalagmites in a high-alpine environment provides irrefutable evidence of liquid water and non-freezing conditions in the shallow subsurface. However, active speleothem growth has been reported beneath glacial ice [17,33,65]. Spotl et al. [17] have documented unusual speleothems from the Austrian Alps that record spelean growth that occurred beneath warm-based glaciers. Notably, there is a significant difference between the Austrian Alps speleothems and the SSJM cave stalagmite. Specifically, the SSJM stalagmite records low $\delta^{13}C$ values due to biogenic CO_2, unlike the remarkable Austrian Alps stalagmites and other speleothems that occur beneath glacial ice which do not record low $\delta^{13}C$ values. The low $\delta^{13}C$ values strongly suggest the presence of surface vegetation, soil, or decaying vegetation at the time of spelean calcite precipitation. Additionally, the strong luminescence of the ~13.5 ka calcite in the SSJM stalagmite indicates the presence of soil-derived HA and FA.

A Hendy test was conducted and revealed minimal variation in oxygen isotope ratios along the same stalagmite growth layer used in the U-series age determination. Oxygen isotope ratios along the ~13.5 ka stalagmite growth layer (Figure 4) indicate that the stalagmite growth layer was in isotopic equilibrium with the drip water that formed the stalagmite. Numerous studies have shown that oxygen and carbon isotopes precipitated under equilibrium conditions, faithfully record both short and long term climate variability [13,17,25,28,66].

The onset of the global Bølling/Allerød warming event was notably fast [50]. At the climate transition, Greenland $\delta^{18}O$ data show a ~10 ºC increase in MAAT within a few years [67]. If a similar and sustained increase in MAAT occurred during the Bølling/Allerød at the study site, surface temperatures would likely have produced rapid glacial ice loss; plant cover and soil development along southern aspects could have become established by ~13.5 ka after the ice cover had melted and exposed the ground surface. This supposition is supported by the C isotope values in the stalagmite. C isotope values in stalagmites principally reflect either the isotopic composition of the bedrock or lowered ^{13}C values derived from oxidation of organic matter in the soil [13,16]. The $\delta^{13}C$ values in the SSJM stalagmite calcite are notably depleted relative to the $\delta^{13}C$ values of the host carbonate (Pennsylvanian Hermosa Group). Lacking soil-derived CO_2, the main contribution of ^{13}C would be from the host carbonate and the $\delta^{13}C$ values in the stalagmite would mimic the $\delta^{13}C$ values of the host carbonate. Additionally, no preserved subaerial exposure surfaces in the Pennsylvanian Hermosa Group were identified in the area near or directly above the SSJM cave during reconnaissance geologic mapping. Preserved subaerial exposure surfaces can be another potential source of lowered ^{13}C values (in shallow caves) that have been largely overlooked in speleothem literature. Subaerial exposure surfaces in ancient carbonate systems are common and can be recognized by diagnostic features and stable isotope patterns [68–71]. ^{13}C-depleted carbon

precipitated in ancient carbonate by the same processes that occur in modern surface soil horizons (i.e., ^{13}C-depleted organic CO_2 produced by plants dissolves in meteoric water which seeps through the soil horizons and re-precipitates carbonate under conditions of subaerial exposure [72] in either upland or lowland karst environments). Since no other reasonable isotopic depletion mechanism exists at the study site, and the Hendy test results indicate that calcite precipitation likely occurred under isotopic equilibrium conditions, the low $\delta^{13}C$ values plausibly indicate the presence of some soil-CO_2 derived ^{13}C at ~13.5 ka.

6.3. Stalagmite fabric

Spelean carbonate petrography was utilized to help determine the nature of the stalagmite growth layers and better understand the depositional history of the layers as it pertains to U-series dates. The micromorphology and microstructure of the SSJM stalagmite shows areas of: (1) minor *dendritic* fabric (*D*-fabric; Figure 8); and, (2) compact *columnar* fabric (*C*-fabric) that has not masked calcite growth layers (Figure 9).

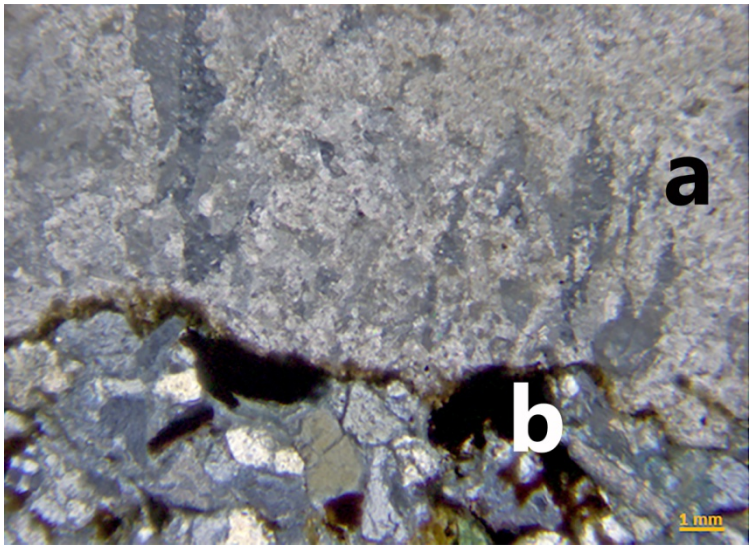

Figure 8. D-fabric (a) is likely characterized by slightly higher drip water episodes alternating with periods of slower (or lesser volume) drip water episodes [73]. D-fabric was observed in the SSJM stalagmite near and adjacent to the host Pennsylvanian Hermosa Group bedrock (b). The D-fabric intermittently continues throughout the oldest ~13.5 ka stalagmite segment. Scale bar is 1mm.

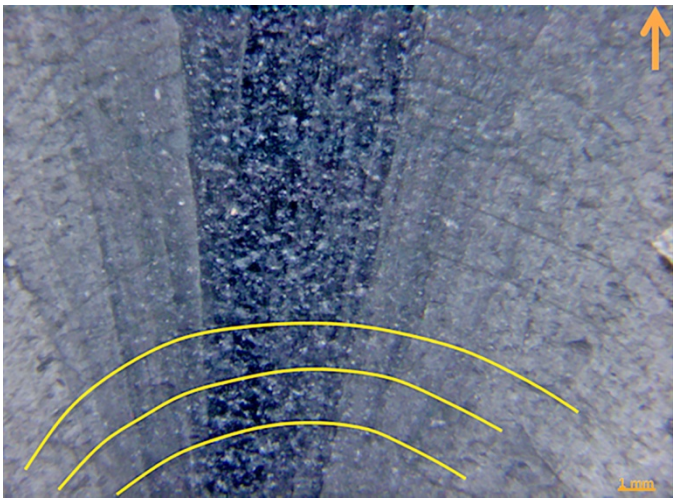

Figure 9. Oriented photomicrograph illustrating compact columnar fabric (C-fabric) along with growth layers (yellow highlighted curved lines). C-fabric is commonly characterized by competitive growth resulting in a parallel arrangement of prismatic, aggregate calcite crystals [74,75] with welded crystal boundaries. C-fabric occurs in the ~13.3 ka stalagmite segment along with visible growth bands. Annual growth band thicknesses in the ~13.5 ka and ~13.3 ka stalagmite sections measure ~1.0 mm thick up to a maximum thickness of ~1.25 mm. The growth band thicknesses in the SSJM stalagmite likely indicate a slightly elevated drip water supply rate. Scale bar is 1 mm.

Crystal fabrics in speleothems are a function of flow rate [76] and therefore record volume changes in drip water through time. Frisia et al. [73], in a comparison study of modern and Holocene microcrystalline fabrics, further demonstrated that D-fabric is characterized by rapid drip episodes alternating with periods of slow drip. Rapid drip episodes are characterized by increased drip flow volumes which are less than higher volume, threshold drip flows which result in under-saturation and corrosion of the bounding layers. D-fabric was observed in the SSJM stalagmite near and adjacent to the host carbonate bedrock (Figure 8), and intermittently continue throughout the oldest ~13.5 ka stalagmite segment. Frisia et al. [73] noted that D-fabric in high-elevation speleothems from the Alps of northeastern Italy and southwestern Ireland were relatively common in the Holocene, but less common in modern stalagmites. As a climate warms and transitions from a glacial maximum, snow and ice cover from the mountain ice caps decrease and the subsequent surface and subsurface discharges fluctuate [77,78]. The flux varies directly with rainfall, surface melt, and solar insolation [77,79,80]. Based on work done by Frisia et al. [73] it is under these conditions that D-fabrics are produced. Previous research has also shown that calcite that formed under equilibrium conditions and precipitated under cold climate conditions often exhibits variable $\delta^{18}O$ composition [81]. The Hendy test that was conducted along the ~13.5 ka growth band revealed minimal variation in oxygen isotope ratios indicating that disequilibrium conditions were not a concern. However, because complementary proxy data is not available, less emphasis has been placed on interpreting climate signals from oxygen isotope values in the SSJM spelean carbonate.

C-fabric is commonly characterized by competitive growth resulting in a parallel arrangement of prismatic, aggregate calcite crystals [74,75] with welded crystal boundaries. C-fabric occurs in the ~13.3 ka stalagmite along with visible growth lines (Figure 9). C-fabrics apparently form under relatively constant drip water conditions [73,82,83] which suggests that relatively constant drip water discharge was likely present when the ~13.3 ka stalagmite segment was precipitating. Spot X-ray powder diffraction analyses consistently showed that the SSJM cave stalagmite is composed of crystalline calcite.

6.4. Annual growth band thickness

Thickness of spelean growth bands is a function of seepage water supply rates and the chemical kinetics of calcite precipitation [72]. Thicker growth bands indicate greater sustained drip water conditions, while thinner layers are indicative of lower seepage supply rates, possibly resulting from slightly drier climate conditions [84]. Qualitative and quantitative annual precipitation levels can be estimated based on spelean growth band thickness [85–87]. Annual growth band thicknesses in the ~13.5 ka and ~13.3 ka stalagmite sections measure ~1.0 mm thick (Figure 9) up to a maximum thickness of ~1.25 mm. For comparison, growth band thickness from a shallow cave speleothem in south Oman varied up to a maximum 0.76 mm [87] during high volume summer monsoon cycles. The growth band thicknesses in the SSJM stalagmite seem to indicate a consistently higher drip water supply rate in the ~13.5 ka and ~13.3 ka stalagmite sections perhaps signaling a period of increased and sustained effective moisture.

6.5. Paraglacial plant succession

Pioneer or seral plant succession in paraglacial landscapes is typically rapid [88]. The rate of change in vegetation classes in early successional stages is similarly elevated during postglacial landscape recovery [88]. Pioneer species improve soil conditions and make habitat suitable for other plants. Rapid glacial retreat in Glacier Bay National Park and Preserve (Alaska) is well-documented and provides a model research area for investigating rapid vegetation response studies and the development of newly created ecosystems in a paraglacial environment. Morris et al. [89] have shown that peat initiation coincided with regional *summer* temperature first rising above 0 ºC. Pioneer plant succession after deglaciation in Glacier Bay (Alaska) document that the successional replacement series (moss to pioneer forbs to cushion plants to semi-erect and erect shrubs and immature coniferous forests) was all accomplished within a span of a century [90,91]. Milner et al. [92] also showed that cyanobacteria, bryophytes and lichen, although still influenced by the nearby glacial microclimate in Glacier Bay, were well-established within 5–15 years of local deglaciation; between 50 and 150 years after local deglaciation, the terrain was colonized by dense shrub thickets. A similar time frame for the succession of vascular plants was observed in central Spitsbergen [93]. The rate at which the plant species number per relevé dramatically increased during the retreat of the near-equatorial Tyndall Glacier (Mt. Kenya, Africa). The rate of successional plant replacement effectively mimicked the rate of glacial retreat (~2.9–3.0 m/yr) [94]. Collectively, these seral plant succession studies have shown that vascular plant colonization of paraglacial environments occurs

rapidly. The stable isotope data from this study suggests that favorable microclimate conditions existed in ice-free areas which allowed subalpine soil and plants to become established; Th/U dates indicate that local paraglacial environments were established prior to ~13.5 ka.

6.6. Deglaciation and research implications

Deglaciation of the Animas Glacier (Figure 2) from the LGM (Pinedale equivalent; MIS 2) terminal position appears to have begun around 19.4 ± 1.5 ka [9] determined from cosmogenic dating of terrace sediments north of Durango, Colorado [9]. Comparable CN ages of initial deglaciation determined from terminal moraine boulders deposited by the Lake Creek Glacier, Colorado (Upper Arkansas River Valley, ~175 km northeast of the study site) yielded a CN age of 19.7 ± 0.5 ka [95]. Young et al. [12] in a comprehensive study of the Lake Creek, Pine Creek, and Clear Creek glaciers (Upper Arkansas River Valley) determined that terminal moraine abandonment began ca. 19.3 ka. CN ages on terminal moraine boulders deposited by the Rio Grande Glacier (Figure 2) yielded a mean age of 18.9 ka [7]. CN exposure dates on LGM terminal moraine boulders from the Mount Massive glacier (central Colorado; ~190 km north-northeast of this site) yielded an age of 19.5 ± 1.77 ka [11]. The onset of near-synchronous deglaciation in the SSJM and across the Colorado Rocky Mountains undoubtedly coincides with an increase in solar insolation along the mid latitude continental regions [52–54] which also corresponds with significant temperature increases extracted from oxygen isotope values in GRIP ice cores [96]. In the Northern Rocky Mountains, Hostetler and Clark [97] showed that deglaciation showed a variable response to climate but was generally more sensitive to changes in temperature than to changes in precipitation.

The U-series dates, carbon isotopes, and luminescence data in this study indicate that deglaciation (ice-free zones) at the high-elevation (3242 m) study site in the SSJM, had occurred sometime prior to ~13.5 ka. The U-series dates correlate well with other deglaciation studies in the southern and central Colorado Rocky Mountains. CN exposure dates on boulders and bedrock surfaces from Mount Massive (central Colorado; ~190 km north-northeast of this site) indicate that *complete* deglaciation of the upper cirque basin (~3,780 m) occurred by ~13 ka [11]. Cirque basins in the Upper Arkansas River Valley (Lake Creek Valley, ~175 km northeast of this site) were also wholly deglaciated by 13.2 ± 0.3 ka [12]. Young et al. [12] have suggested that a near-synchronous demise of all mountain glaciers across the western USA was achieved between ca. 15 ka and ca. 13 ka. The SSJM cave is at a lower latitude and lower elevation than the Mount Massive and Upper Arkansas River Valley glacial cirque studies and has a southern aspect. *A priori*, deglaciation in the SSJM should have occurred slightly earlier than higher elevation and more northerly latitude sites in the southern Rocky Mountains. Regardless, the U-series date for the SSJM stalagmite falls within the error range for *complete* deglaciation at Mount Massive [11] and in the Upper Arkansas River Valley cirques [12]. Collectively, data from these deglaciation studies enhances the confidence level that the area above the SSJM cave was deglaciated prior to ~13.5 ka.

Guido et al. [9] using CN dating of exposure surfaces in the Animas River Valley established a SSJM deglaciation rate of ~15.4 m/year and have suggested that “complete” deglaciation in the SSJM occurred by ~12.3 ka ± 1 ka. The ~12.3 ka ± 1 ka date was obtained from glacially-polished bedrock in a north-facing cirque (~9.5 km east/northeast of the cave at an elevation of ~3700 m

which is ~460 m higher than the site in this study). Although the ~12.3 ka date may represent complete deglaciation in the SSJM, the authors state that their glacial "retreat" history indicates that the fastest deglaciation episode likely occurred between 16–13 ka [9]. The Th/U ages presented herein support the inference by Guido et al. [9] of rapid glacial retreat. Guido et al. [9] further speculate that this rapid retreat phase may be linked to a regional climate shift that ushered in elevated temperature and/or decreased precipitation. Oviatt et al. [98] in a study of pluvial Lake Bonneville (a series of large, connected topographically-closed structural basins in the eastern Great Basin, ~500 km west/northwest of the study site) documented rapid lake desiccation and a catastrophic lake level depression of 100 m between 14.5–12 ka. These rapid, regional temperature/aridity changes likely impacted the rate of deglaciation in the SSJM area. The Th/U spelean ages from this study corroborate a regional climate shift and indicate that deglaciation in the SSJM was not monotonically uniform but spatially heterogeneous. The southern aspect and broad open-area land surface above the cave site was almost certainly a contributing factor to the non-uniform loss of glacial ice cover.

Previous deglaciation studies in the SSJM have predominantly focused on dating the maximum glacial extent and younger features indicative of glacial termination, and the general rate of deglaciation. Progression of mountain glacier retreat is non uniform and is also characterized by considerable glacier oscillation phases and stagnation events [99–101]. The development of a scattered pattern of ice-free land surfaces during deglaciation is influenced by local geomorphic factors including aspect, still-stands, and other glacio-geomorphic features [11,102,103]. Providing robust, quantitative age constraints on areas of ice-free (fenster-like) land surrounded by glacial ice cover is problematic but is necessary in order to better understand the intricacies of glacial evolution and the sensitivity of a retreating glacial system. The glacial evolution of the Animas Glacier in the SSJM is not well known. Th/U results from this study document an unequal distribution of glacial ice cover and early ice-free land surfaces areas, and the Th/U results provide a preliminary quantitative approach to better understand the spatial and temporal dynamics of the complex deglaciation system. Additional quantitative research, similar to this study, will help unravel the evolution of the Animas Glacier and similar mountain glaciers.

7. Summary and conclusions

The growth of stalagmites in a high-alpine environment provides irrefutable evidence of liquid water and non-freezing conditions in the shallow subsurface. U-series dates from long transects along continuous stalagmite growth bands in a cave near Molas Pass in the SSJM (Colorado, USA) indicate that speleothem growth began ~13.446 ± 0.170 ka during the warm, moist Bølling/Allerød interstadial (~14.6–12.9 ka). Stalagmite growth ceased at 13.284 ± 0.180 ka just prior to the onset of the YD stadial (~12.9 ka). A significant time gap occurred between 13.284 ± 0.180 ka and 2.666 ± 0.503 ka. Renewed stalagmite growth at 2.666 ± 0.503 ka appears to correlate with a distinctly wetter and cooler climatic optimum that existed in southwestern USA from 3.0 ka to 8.0×10^{-1} ka and from 2.6 ka in the SSJM based on pollen records preserved in a nearby lake. The Th/U spelean ages from this study corroborate a previously proposed, regional climate shift, and indicate that deglaciation in the SSJM was not monotonically uniform but spatially heterogeneous.

Key geomorphic factors, such as the southern aspect and broad open-area land surface above the cave site, almost certainly were a contributing factor to the unequal distribution of glacial ice cover during deglaciation. Results from this study begin to illustrate the complex nature of spatially heterogeneous ice cover during glacier retreat.

Low ^{13}C values of calcite in the oldest stalagmite growth layers, relative to the ^{13}C values of the host Hermosa Group carbonate, indicate that soil and vegetation were likely present at the surface, at the elevation of the study site (~3242 m) prior to 13.5 ka. Strong, light green luminescence of the oldest stalagmite growth layers under SWUV light indicate the presence of HA and FA which similarly indicate that soil and vegetation were likely present at the surface above the cave. Collectively these data indicate that the land surface above the SSJM cave was glacier-free by ~13.5 ka and these data also support the unequal or non-uniform loss of glacial ice cover (spatial heterogeneity) that occurred during glacial retreat.

Acknowledgments

Carbon and oxygen isotope ratios were obtained from the Colorado Plateau Stable Isotope Lab at Northern Arizona University and at the Center for Stable Isotope Mass Spectrometry at the University of Texas at Austin. U-series dates were performed at the University of Texas at Austin (special thanks to Drs. Banner, James, and Loewy). Thanks to Mimi Moller for some microscope work related to this project. Funding for this research was supplied by the author and a Traditional Scholarship and Research Grant from Fort Lewis College. Permission to enter and sample in the SSJM cave was authorized under USFS entry permit 13-13-001; USFS decontamination protocol for *Geomyces destructans* was strictly adhered to prior to cave entry and after the cave research was completed. Multiple internal and anonymous external reviewers provided helpful comments that improved the manuscript.

Conflict of interest

The author declares that there is no conflict of interest associated with this research.

References

1. Andrews JT, Carrara PE, King FB, et al. (1975) Holocene environmental changes in the Alpine Zone, Northern San Juan Mountains, Colorado: Evidence from Bog stratigraphy and palynology. *Quat Res* 5: 173–197.
2. Petersen KL, Mehringer PJ (1976) Postglacial timberline fluctuations, La Plata Mountains, Southwestern Colorado. *Arct Alp Res* 8: 275–288.
3. Carrara PE, Mode WN, Rubin M, et al. (1984) Deglaciation and postglacial timberline in the San Juan Mountains, Colorado. *Quat Res* 21: 42–55.
4. Friedman I, Carrara P, Gleason J (1988) Isotopic evidence of Holocene climatic change in the San Juan Mountains, Colorado. *Quat Res* 30: 350–353.

5. Elias SA, Carrara PE, Toolin LJ, et al. (1991) Revised age of deglaciation of Lake Emma based on new radiocarbon and macrofossil analysis: *Quat Res* 36: 307–321.
6. Gillam ML (1998) Late Cenozoic geology and soils of the Lower Animas River Valley, Colorado and New Mexico: Boulder. University of Colorado, 477.
7. Benson L, Madole R, Landis G, et al. (2005) New data for late Pleistocene Pinedale glaciation from southwestern Colorado. *Quat Sci Rev* 24: 49–65.
8. Toney JL, Anderson RS (2006) A postglacial palaeoecological record from the San Juan Mountains of Colorado USA: fire, climate and vegetation history. *Holocene* 16: 505–517.
9. Guido ZS, Ward DJ, Anderson RS (2007) Pacing the post-Glacial Maximum demise of the Animas Valley glacier and the San Juan Mountain ice cap, Colorado. *Geology* 35: 739–742.
10. Ward DJ, Anderson RS, Guido ZS, et al. (2009) Numerical modeling of cosmogenic deglaciation records, Front Range and San Juan mountains, Colorado. *J Geophys Res Earth Surface* 114: F01026.
11. Mason C, Ruleman CA, Kenny R (2011) Rate and timing of deglaciation using ^{10}Be cosmogenic nuclide surface exposure dating, Mt. Massive Wilderness, Colorado, USA. *Geol Soc Am Abst Prog* 43: 65.
12. Young NE, Briner JP, Leonard EM, et al. (2011) Assessing climatic and nonclimatic forcing of Pinedale glaciation and deglaciation in the western United States. *Geology* 39: 171–174.
13. Dorale JA, Edwards RL, Ito E, et al. (1998) Climate and vegetation history of the midcontinent from 75 to 25 ka: a speleothem record from Crevice Cave, Missouri, USA. *Science* 282: 1871–1874.
14. Dorale JA, Edwards RL, Alexander EC Jr, et al. (2001) Uranium-series dating of speleothems: Current techniques, limits, and applications. In: Sasowsky ID, Mylroi JE (eds), *Study of Cave Sediments: Physical and Chemical records of palaeoclimate*, Newark: Kluwar/Plenum, 177–197.
15. Richards DA, Dorale JA (2003) Uranium-series chronology and environmental applications of speleothem. *Rev Mineral Geochem* 52: 407–460.
16. Asmerom Y (2009) Speleothems, In: Gornitz V (ed), *Encyclopedia of Paleoclimatology and ancient environments*, The Netherlands, Springer, 916–918.
17. Spötl C, Mangini A, Richards DA (2006) Chronology and paleoenvironment of Marine Isotope Stage 3 from two high-elevation speleothems, Austrian Alps. *Quat Sci Rev* 25: 1127–1136.
18. Hendy CH (1971) The isotopic geochemistry of speleothems, I. The calculation of the effects of different modes of formation on the isotopic composition of speleothems and their applicability as paleoclimatic indicators. *Geochem Cosmochem Acta* 35: 801–824.
19. Spötl C, Mangini A (2002) Stalagmite from the Austrian Alps reveals Dansgaard-Oeschger events during isotope stage 3: Implications for the absolute chronology of Greenland ice cores. *Earth Planet Sci Lettr* 203: 507–518.
20. Moseley GE, Spötl C, Svensson A, et al. (2014) Multi-speleothem record reveals tightly coupled climate between central Europe and Greenland during Marine Isotope Stage 3. *Geology* 42: 1043–1046.
21. Dykoski CA, Edwards RL, Cheng H, et al. (2005) A high-resolution, absolute-dated Holocene and deglacial Asian monsoon record from Dongge Cave, China. *Earth Planet Sci Lett* 233: 71–86.

22. Neff U, Burns SJ, Mangini A, et al. (2001) Strong coherence between solar variability and the monsoon in Oman between 9 and 6 kyr ago. *Nature* 411: 290–294.
23. Berstad IM, Lundberg J, Lauritzen SE, et al. (2002) Comparison of the climate during Marine Isotope Stage 9 and 11 inferred from a speleothem isotope record from northern Norway. *Quat Res* 58: 361–371.
24. Wang Y, Cheng H, Edwards RE, et al. (2005) The Holocene Asian monsoon: links to solar changes and North Atlantic climate. *Science* 308: 854–857.
25. Mangini A, Spötl C, Verdes P (2005) Reconstruction of temperature in the Central Alps during the past 2000 years from a $\delta^{18}O$ stalagmite record. *Earth Planet Sci Lettr* 235: 741–751.
26. Genty D, Blamart D, Ouahdi R, et al. (2003) Precise dating of Dansgaard-Oeschger climate oscillations in western Europe from stalagmite data. *Nature* 421: 833–837.
27. Denniston RF, González LA, Asmerom Y, et al. (2000) Speleothem records of early and late Holocene vegetation dynamics in the Ozark Highlands, USA. *Quat Int* 67: 21–27.
28. McDermott F (2004) Palaeo-climate reconstruction from stable isotope variations in speleothems: A review. *Quat Sci Rev* 23: 901–918.
29. Atwood WW, Mather KF (1932) *Physiography and Quaternary geology of the San Juan Mountains, Colorado.* Washington, D.C.: USGS Prof Paper 166: 176.
30. Porter SC, Pierce KL, Hamilton TD (1983) Late Wisconsin mountain glaciation in the western United States, In: Porter SC (ed), *Late Quaternary environments of the United States, v. 1, The late Pleistocene*, Minneapolis: U of Minnesota Press: 1–111.
31. Benson L, Madole R, Phillips W, et al. (2004) The probable importance of snow and sediment shielding on cosmogenic ages of north-central Colorado Pinedale and pre-Pinedale moraines. *Quat Sci Rev* 23: 193–206.
32. Medville D (2001) The exploration and survey of Surprise Cave. *NSS News* 59: 288–289.
33. Atkinson TC (1983) Growth mechanisms of speleothems in Castleguard Cave, Columbia Icefields, Alberta, Canada. *Arct Alp Res* 15: 523–536.
34. Rangwala I (2008). 20th Century Climate Change: Chapter 5, The San Juan Mountains in Southwest Colorado: Investigating long term trends in climate and hydrological variables and explaining the causes for a rapid climate change in the region between 1985–2005: New Jersey, Rutgers University, 35.
35. Ray AJ, Barsugli JJ, Averyt KB (2008) Climate change in Colorado: A synthesis to support water resources management and adaptation: Western Water assessment for Colorado Water Conservation, Paper 53. Available from: http://cwcb.state.co.us/Home/ClimateChange/ClimateChangeInColoradoReport/
36. Mote PW, Hamlet AF, Clark M, et al. (2005) Declining mountain snowpack in western North America. *Bull Am Meteorol Soc* 86: 39–49.
37. Clow D (2008) Changes in the Timing of Snowmelt in Colorado. In: *Presentation at the 50th Annual Convention of the Colorado Water Congress, January*: 23–25.
38. Carrara PE (2011) *Deglaciation and Postglacial treeline fluctuation in the Northern San Juan Mountains, Colorado*. Washington, D.C.: USGS Prof Paper 1782: 48.
39. Musgrove M, Banner JL, Mack LE, et al. (2001) Geochronology of late Pleistocene to Holocene speleothems from central Texas: Implications for regional paleoclimate. *GSA Bull* 113: 1532–1543.

40. Fanditis J, Ehhalt DH (1970) Variations of the carbon and oxygen isotopic composition in stalagmites and stalactites: Evidence of non-equilibrium isotopic fractionation. *Earth Planet Sci Lett* 10: 136–144.
41. Gascoyne M, Schwarcz HP, Ford DC (1980) A palaeotemperature record for the mid-Wisconsin in Vancouver Island. *Nature* 285: 474–476.
42. Polyak VJ, Asmerom Y (2001) Late Holocene climate and cultural changes in the southwestern United States. *Science* 294: 148–151.
43. Gilson JR, Macarthney E (1954) Luminescence of speleothems from Devon, UK: the presence of organic activators (abs). *Ashford Speleo Soc J* 6: 8–11.
44. Lauritzen SE, Ford DC, Schwarcz HP (1986) Humic substances in speleothems matrix-paleoclimatic significance. Proceedings of 9th International Congress of Speleology, Barcelona, 2: 77–79.
45. Shopov YY (2001) Luminescence of cave minerals. *Bull Venezuelan Speleo Soc* 35: 27–33.
46. White WB, Brennan ES (1989) Luminescence of speleothems due to fulvic acid and other activators. Proceedings of 10th International Congress of Speleology, Budapest 1: 212–214.
47. Shopov YY (1997) Luminescence of cave minerals. In: Hill C, Forti P (eds), *Cave Minerals of the World*, 2nd Ed, Huntsville, Alabama: National speleological society, 244–248.
48. Ford DC (1997) Dating and Paleo-environmental studies of speleothems. In: Hil C, Forti P (eds), *Cave Minerals of the World*, 2nd Ed, Huntsville, Alabama: National speleological society: 271–284.
49. McGarry SF, Baker A (2000) Organic acid fluorescence: applications to speleothem palaeoenvironmental reconstruction. *Quat Sci Rev* 19: 1087–1101.
50. Thiagarajan N, Subhas AV, Southon JR, et al. (2014) Abrupt pre-Bølling–Allerød warming and circulation changes in the deep ocean. *Nature* 511: 75–78.
51. Feng W, Hardt BF, Banner JL, et al. (2014) Changing amounts and sources of moisture in the U.S. southwest since the Last Glacial Maximum in response to global climate change. *Earth Planet Sci Lett* 401: 47–56.
52. Cheng H, Edwards RL, Broecker WS, et al. (2009) Ice age terminations. *Science* 326: 248–252.
53. Denton GH, Anderson RF, Toggweiler JR, et al. (2010) The last glacial termination. *Science* 328: 1652–1656.
54. Broecker WS, Denton GH (1990) The role of ocean-atmosphere reorganizations in glacial cycles. *Quat Sci Rev* 9: 305–341.
55. Barrows TT, Juggins S, De Deckker P, et al. (2007) *Paleoceanography* 22: PA2215.
56. Asmerom Y, Polyak V, Burns S, et al. (2007) Solar forcing of Holocene climate; new insights from a speleothem record, Southwestern United States. *Geology* 35: 1–4.
57. Lachniet MS, Denniston RF, Asmerom Y, et al. (2014) Orbital control of western North America atmospheric circulation and climate over two glacial cycles. *Nat Commun* 5: 3805.
58. Rasmussen SO, Andersen KK, Svensson AM, et al. (2006) A new Greenland ice core chronology for the last glacial termination. *J Geophys Res Atmos* 111: 6.
59. Linge H, Baker A, Andersson C, et al. (2009) Variability in luminescent lamination and initial $^{230}Th/^{232}Th$ activity ratios in a late Holocene stalagmite from northern Norway. *Quat Geochronol* 4: 181–192.

60. Rajendran CP, Sanwal J, Morell KD, et al. (2016) Stalagmite growth perturbations from the Kumaun Himalaya as potential earthquake recorders. *J Seismol* 20: 579–594.
61. Railsback LB, Akers PD, Wang L, et al. (2013) Layer-bounding surfaces in stalagmites as keys to better paleoclimatological histories and chronologies. *Int J Speleol* 42: 167–180.
62. Stock GM, Granger DE, Sasowsky ID, et al. (2005) Comparison of U–Th, paleomagnetism, and cosmogenic burial methods for dating caves: implications for landscape evolution studies. *Earth Planet Sci Lett* 236: 388–403.
63. Polyak VJ, Asmerom Y (2001) Late Holocene climate and cultural changes in the southwestern United States. *Science* 294: 148–151.
64. Asmerom Y, Polyak VJ, Burns SJ (2010) Variable winter moisture in the southwestern United States linked to rapid glacial climate shifts. *Nat Geosci* 3: 114–117.
65. Harmon RS, Ford DC, Schwarcz HP (1977) Interglacial chronology of the Rocky and Mackenzie Mountains based upon ^{230}Th–^{234}U dating of calcite speleothems. *Can J Earth Sci* 14: 2543–2552.
66. Fairchild IJ, Baker A (2012) *Speleothem Science*. Chichester, Wiley-Blackwell: 432.
67. Steffensen JP, Andersen KK, Bigler M, et al. (2008) High-Resolution Greenland Ice Core Data Show Abrupt Climate Change Happens in Few Years. *Science* 321: 680–684.
68. Kenny R, Neet KE (1993) Upper Pennsylvanian-Permian (Naco Group) paleosols (north-central Arizona): field and isotopic evidence. *Geoderma* 58: 131–148.
69. Kenny R, Knauth LP (2001) Stable isotope variations in the Neoproterozoic Beck Spring Dolomite and Mesoproterozoic Mescal Limestone paleokarst: Implications for life on land in the Precambrian. *GSA Bull* 113: 650–658.
70. Allan JR, Matthews RK (1982) Isotopic signatures associated with early meteoric diagenesis. *Sedimentology* 29: 797–817.
71. Beeunas MA, Knauth LP (1985) Preserved stable isotope signature of subaerial diagenesis in the 1.2-b.y. Mescal Limestone, central Arizona: Implications for the timing and development of a terrestrial plant cover. *GSA Bull* 96: 737–745.
72. Dreybrodt W (1999) Chemical kinetic, speleothem growth and climate. *Boreas* 28: 347–356.
73. Frisia S, Borsato A, Fairchild IJ, et al. (2000) Calcite fabrics, growth mechanisms, and environments of formation in speleothems from the Italian Alps and southwestern Ireland. *J Sed Res* 70: 1183–1196.
74. Onac B (1997) Crystallography of Speleothems, In: Hill C, Forti P (eds.) *Cave Minerals of the World,* 2nd Ed, Huntsville, Alabama: National Speleological Society, 230–235.
75. Kendall AC, Broughton PL (1978) Origin of fabrics in speleothems composed of columnar calcite crystals. *J Sed Res* 48: 519–538.
76. Gonzales LA, Carpenter SJ, Lohmann KC (1992) Inorganic calcite morphology: roles of fluid chemistry and fluid flow. *J Sed Petrol* 62: 383–399.
77. Fountain AG, Walder JS (1998) Water flow through temperate glaciers. *Rev Geophys* 36: 299–328.
78. Hock R, Jansson P, Braun LN (2005) Modelling the response of mountain glacier discharge to climate warming, In: Huber UM, Bugmann HKM, Reasoner MA (eds.) *Global change and mountain regions (A state of knowledge overview)*, Springer, Dordrecht, 243–252.
79. Hodson A, Anesio AM, Tranter M, et al. (2008) Glacial ecosystems. *Ecol Monogr* 78: 41–67.

80. Bates B, Kundzewicz ZW, Wu S, et al. (2008) *Climate change and water. Technical paper of the Intergovernmental Panel on Climate Change*, Geneva: IPCC Secretariat, 210.
81. Lacelle D (2007) Environmental setting, (micro) morphologies and stable C–O isotope composition of cold climate carbonate precipitates—a review and evaluation of their potential as paleoclimatic proxies. *Quat Sci Rev* 26: 1670–1689.
82. Turgeon S, Lundberg J (2001) Chronology of discontinuities and petrology of speleothems as paleoclimatic indicators of the Klamath Mountains, southwest Oregon, USA. *Carb Evap* 16: 153–167.
83. Frisia S (2015) Microstratigraphic logging of calcite fabrics in speleothems as tool for palaeoclimate studies. *Int J Speleo* 44: 1–16.
84. Brook GA, Railsback LB, Cooke HJ, et al. (1992) Annual Growth Layers in a Stalagmite from Drotsky's Cave, Ngamiland: Relationships between layer thickness and precipitation. *Botsw Notes Rec* 24: 151–63.
85. Burns SJ, Fleitmann D, Mudelsee M, et al. (2002) A 780-year annually resolved record of Indian Ocean monsoon precipitation from a speleothem from south Oman. *J Geophys Res* 107: 4434.
86. Baker A, Smart PL, Edwards RL, et al. (1993) Annual growth banding in cave stalagmite. *Nature* 304: 518–520.
87. Fleitmann D, Burns SJ, Neff U, et al. (2004) Palaeoclimate interpretation of high-resolution oxygen isotope profiles derived from annually laminated speleothems from southern Oman. *Quat Sci Rev* 23: 935–945.
88. Klaar MJ, Kidd C, Malone E, et al. (2015) Vegetation succession in deglaciated landscapes: implications for sediment and landscape stability. *Earth Surf Process Landf* 40: 1088–1100.
89. Morris PJ, Swindles GT, Valdes PJ, et al. (2018) Global peatland initiation driven by regionally asynchronous warming. *Proc Natl Acad Sci USA* 115: 4851–4856.
90. Lawrence DB, Schoenike RE, Quispel A, et al. (1967) The role of Dryas drummondii in vegetation development following ice recession at Glacier Bay, Alaska, with special reference to its nitrogen fixation by root nodules. *J Ecol*: 793–813.
91. Lawrence DB (1958) Glaciers and vegetation in south-eastern Alaska. *Am Sci* 46: 138A–122.
92. Milner AM, Fastie CL, Chapin FS, et al. (2007) Interactions and linkages among ecosystems during landscape evolution. *BioSci* 57: 237–247.
93. Prach K, Rachlewicz G (2012) Succession of vascular plants in front of retreating glaciers in central Spitsbergen. *Polish Polar Res* 33: 319–328.
94. Mizuno K (2005) Glacial fluctuation and vegetation succession on Tyndall Glacier, Mt Kenya. *Mtn Res Develop* 25(1): 68–76.
95. Schildgen T (2000) Fire and ice: Geomorphic history of Middle Boulder Creek as determined by isotopic dating techniques. CO Front Range: Williamstown, Massachusetts, Williams College: 30.
96. Johnsen SJ, Clausen HB, Dansgaard W, et al. (1997) The δ18O record along the Greenland Ice Core Project deep ice core and the problem of possible Eemian climatic instability. *J Geophys Res (Oceans)* 102: 26397–26410.
97. Hostetler SW, Clark PU (1997) Climatic controls of western US glaciers at the last glacial maximum. *Quat Sci Rev* 16: 505–511.

98. Oviatt CG, Currey DR, Sack D (1992) Radiocarbon chronology of Lake Bonneville, eastern Great Basin, USA. *Palaeogeogr Palaeoclimatol Palaeoecol* 99: 225–241.
99. Butler D (1986) Pinedale deglaciation and subsequent Holocene environmental changes and geomorphic responses in the central Lemhi Mountains, Idaho, USA. *Géogr Phys Quat* 40: 39–46.
100. Thackray GD, Lundeen KA, Borgert JA (2004) Latest Pleistocene alpine glacier advances in the Sawtooth Mountains, Idaho, USA: reflections of midlatitude moisture transport at the close of the last glaciation. *Geology* 32: 225–228.
101. Serrano E, González-Trueba JJ, Pellitero R, et al. (2013) Quaternary glacial evolution in the Central Cantabrian Mountains (northern Spain). *Geomorphology* 196: 65–82.
102. Smedley RK, Glasser NF, Duller GAT (2016) Luminescence dating of glacial advances at Lago Buenos Aires (~46 S), Patagonia. *Quat Sci Rev* 134: 59–73.
103. Friele PA, Clague JJ (2002) Younger Dryas readvance in Squamish river valley, southern Coast mountains, British Columbia. *Quat Sci Rev* 21: 1925–1933.

AIMS Press